Investigation of Heat Treatment and Friction Stir Processing Effects on Mechanical Properties and Micro Structural Evolution of Sc-Inoculated Al-Zn-Mg Alloys

Dr. J. MURALI NAIK
Associate Professor,
Department of Mechanical Engineering,
Holy Mary Institute of Technology and Science,
Bogaram (v), Keesara(m), Medchal Dist, Hyderabad, Telangana-501301

ABSTRACT
This study investigates the effects of various artificial ageing parameters on Vickers hardness characteristics and the surface modification of scandium inoculated Al-Zn-Mg alloys through friction stir processing. The aluminium alloys were subjected to a solution treatment at 465°C for one hour, followed by quenching in water and artificial ageing at temperatures of 120°C, 140°C, and 180°C for varying durations up to twenty hours. In addition, friction stir processing was used to address casting porosity and refine cast microstructures. These microstructural changes resulted in a significant improvement in both the strength and ductility of the aluminium alloys (7xxx series). Generally, a high tool rotation rate proved beneficial in breaking down coarse second-phase particles, healing casting porosity, homogenizing the material, and consequently increasing strength. Thus, friction stir processing was adopted for microstructure modification in cast aluminium alloys to refine grain structure and enhance mechanical properties.

Keywords: Fine Microstructures, Solutionizing, Artificial Ageing, Inoculation and Friction Stir Processing

1. INTRODUCTION

Heat treatment is an important process in the final fabrication of any engineering component. The goal of heat treatment is to enhance the structural and physical properties of the metal for a specific application. Solution heat treatment, a type of heat treatment for aluminum alloys, allows for the maximum concentration of hardening solute to dissolve into the solution by heating the alloy to a temperature that creates a single phase. After holding the alloy for a sufficient amount of time to ensure complete homogeneity, it is rapidly quenched to prevent solute atoms from precipitating out of solution. As a result, a super-saturated solution is formed between the solute atoms in the aluminum matrix. Precipitation strengthening solid solutions involve the formation of finely dispersed precipitates during aging heat treatment, which can occur naturally or artificially. The aging process must be performed below the equilibrium solvus temperature and below a metastable miscibility gap known as the Guinier-Preston (GP) zone solvus line [1-10]. The Al-Zn-Mg (7xxx series) is a heat-treatable alloy that exhibits a strong aging response when suitable temperature and time are provided to form stable η phase and its precursors. These alloys benefit from precipitation strengthening through complex decomposition processes involving both stable and metastable phases, which has industrial advantages. In the Al-Zn-Mg system, the interaction between small zinc atoms and large magnesium atoms on the aluminum lattice, which involves clustering to reduce lattice strain energy, plays a significant role in the decomposition processes during aging [11,12]. However, these alloys are susceptible to stress corrosion cracking (SCC) in the

highest strength temper (T6). Over-aged heat treatment conditions can decrease stress corrosion cracking susceptibility, but it also reduces the strength [13]. Previous literature has pointed out that the precipitation free zone (PFZ) and η (MgZn2) particles are finely dispersed within the grains and accumulated at the grain boundaries, which is responsible for intergranular corrosion. Therefore, the density of fine precipitates, which contributes to the high strength and stress corrosion cracking resistance of the alloy, is generally controlled by the heat treatment. Furthermore, Al-Zn-Mg alloys can be hardened further through the inoculation effect of Sc [14,15]. The addition of Sc results in the formation of Al3Sc dispersoids, which greatly refine grains and inhibit the recrystallization process, leading to enhanced strength and corrosion resistance. By forming Al3Sc particles in aluminum alloys, Sc is known to reduce hot tearing and shrinkage porosity, produce a more uniform microstructure, and retard grain growth through the Zener effect [16]. Scandium forms a limited-solubility eutectic diagram with aluminum (Figure 2) [17]. Inoculating the melt with the Al3Sc (L12-type) phase leads to heterogeneous nucleation of aluminum grains [18]. It has been observed that the average amount of Zn and Mg retained in solid solution within a grain interior is very low. Zn and Mg tend to segregate at grain boundary areas due to partitioning effects during freezing. Since the percentage of The area accounted for by grain boundaries is much higher in the alloys containing Sc, indicating that their partitioning effect must be increased with Sc addition. The sequence of precipitation in aluminium alloys strongly depends on the history of the materials, including quenching conditions, natural ageing, and further heat treatment. Different processes may be involved, such as dissolution, coarsening, or phase transformation from metastable precipitates to a more stable phase. GP zones are formed at low temperatures after quenching, typically at room temperature, and can act as nucleation sites for more stable precipitates. When the temperature is increased from the pre-ageing temperature to the ageing temperature, dissolution of GP zones occurs. This dissolution is called reversion and can be partial. When the ageing temperature is higher than the reversion temperature, the GP zone dissolution is complete. In spite of this complete reversion, ageing can still result in a fine distribution of ή-particles. As η particles are incoherent with the matrix and have a relatively high interfacial energy, metastable precipitates (ή) with a higher level of coherency (and lower interfacial energy) may be expected to form preferentially at lower temperatures due to a lower activation barrier for nucleation. The common metastable phases in the 7xxx system are GP zones and ή particles, respectively.According to the binary phase diagram of Al-Zn (Figure 1), the solubility of the solid solution decreases as the temperature decreases due to the existence of solvus solubility. The decreased solubility of the solid solution leads to its saturation, making the material thermodynamically unstable and predisposed to decompose into two new phases [19].

The effect of the ageing treatment is evaluated through Vicker's hardness testing and metallography. Hardness measurements can provide a good indication of the material strength, and since strength is related to the number, type, and spacing of precipitates, hardness measurements can be used to monitor the precipitation process. Vicker's hardness tests were conducted to analyze the influence of the precipitated phases formed during the ageing treatment on the alloy's hardness. Additionally, tensile testing has been carried out to assess the material's mechanical properties for engineering applications. The examination of the tensile fracture surface can reveal the morphology, size, and mode of fracture of the precipitates, as well as provide information about the alloy's chemistry and heat treatment processes.

In addition, friction-stir processing (FSP) is an emerging surface engineering technology that can eliminate casting defects and improve microstructures locally. This process enhances strength, ductility, corrosion resistance, deformability, and other properties [20]. FSP is a local thermo-mechanical metalworking process that changes properties in a specific area without affecting the rest of the structure [21].During FSP, the tool design and process parameters are optimized. The tool rotation rate is set at 1000 rpm, and the traverse speed is 70 mm/min. The total FSP length is approximately 150 mm, from the pin entry to the pin exit. The tools used include a concave shoulder with a diameter of 20 mm and a conical pin with a root diameter of 5 mm, tip diameter of 3.5 mm, and length of 5 mm.Various tests were

conducted to characterize the material, including Vickers hardness testing, mechanical testing, electron probe microanalysis (EPMA), differential scanning calorimetry (DSC), X-ray diffraction (XRD), field emission scanning electron microscopy (FESEM), scanning electron microscopy (SEM), and transmission electron microscopy (TEM) analysis on the experimental alloys.Lastly, there is a need to emphasize the aspect of heat treatment and surface modification through friction stir processing on cast Al-Zn-Mg alloys with Sc inoculation.

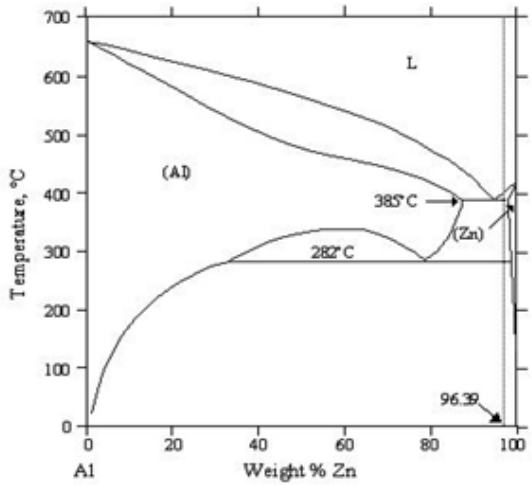

Figure 1. The Al-Zn equilibrium phase diagram

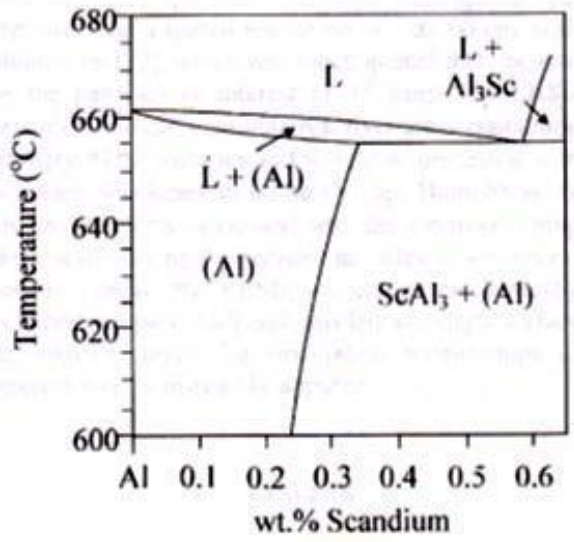

Figure 2. The Al-rich end Al-Sc phase diagram

2. EXPERIMENTAL PROCEDURES:

The four types of aluminium alloys were prepared by cast metallurgy with pure Zn, pure Mg and master alloy Al-2wt.%Sc. Basically, prepared alloys were 7xxx series of Al-Zn-Mg without and with Sc addition. The muffle furnace was used to melt the alloys at 780°C. The melt was cast in an air by a steel mould in plate shape(150×90×8 mm^3). The chemical composition of 7xxx series of aluminium alloys were determined by inductively coupled plasma atomic emission spectroscopy (ICP-AES) and atomic

absorption spectroscopy (AAS) methods and is shown in Table 1. The specimens were subjected to the following heat treatment: solution treatment at 465±5°C for 1 h, followed by quenching in water at roomtemperature then kept for seven days for natural ageing Then, artificial ageing performed at 120±2°C, 140±2°C And 180±2°C, respectively. The metallographic specimens were examined under an optical microscope after etching with a modified Keller's reagent (2.5 ml HNO3+1.5 ml HCl+1 ml HF+ 95 ml water). The as-cast samples were analyzed by electron probe microanalysis (EPMA) with EDS to examine segregation on grain boundaries. Microhardness tests were done with a Vickers diamond indenter with a pyramidal shape with a 10 kg load at different time intervals: 5, 15, 30, 60, 120, 240, 360, 480, 600, 720, 960, and 1200 min. Five measurements were taken randomly for each sample, and the average value and standard deviation were calculated. The hardness values were recorded immediately after aging and continued for twenty hours at the above intervals. The tensile tests were carried out using an Instron testing machine at a crosshead speed of 1 mm/min, as shown in Table 2. The tensile specimen had a 26 mm gauge length, 4 mm width, 2.5 mm thickness, and 58 mm length with a fully processed zone by double passes. During friction stir processing (FSP), the following parameters were controlled to obtain sound, defect-free test plates: a tool rotation rate of 1000 rpm and a traverse speed of 70 mm/min. The total FSP length was around 150 mm, from the pin entry to the pin exit. A tool with a concave shoulder 20 mm in diameter and a conical pin 5 mm in root diameter, 3.5 mm in tip diameter, and 5 mm in length was used. Therefore, in order to obtain fully processed zone plates with double passes, the field emission scanning electron microscopy (FESEM) was used to analyze the phases, along with energy-dispersive spectroscopy to determine their chemical compositions. FESEM was conducted on a QUANTA 200F, 30 kV model. Similarly, the fracture surfaces of tensile specimens were studied by scanning electron microscopy (SEM) analysis, and the as-cast grain size was measured by the mean linear intercept method. The X-ray diffraction (XRD) method was used to identify different beneficial phases of aluminum alloys. The differential scanning calorimeter (DSC) measurements were performed using an EXSTAR TG/DTA 6300 equipment with a 10°C/min heating rate until 600°C in a nitrogen atmosphere on solution-treated and aged samples at 140°C for 6 h. Specimens for transmission electron microscopy (TEM) with a diameter of 3 mm were cut from the as-cast 10×10 mm2 discs and reduced in thickness to 0.1 mm. Then, the TEM samples were prepared using twin-jet electro-polishing (solution was 75% CH3OH and 25% HNO3) at 12 V and -35°C. All the imaging was carried out using a Techai G2 20 S-TWIN at 200 kV.

3. RESULTS AND DISCUSSION:

Aluminum alloys are generally categorized into two classes: heat-treatable and non-heat-treatable alloys. Following the international AA (Aluminium Association) designation, the heat-treatable alloys are the 2xxx series (Al-Cu alloys), the 6xxx series (Al-Mg-Si), and the 7xxx series (Al-Zn-Mg). These alloys derive their strength from artificial aging processes and precipitation hardening. Adding Scandium (Sc) to one of the heat-treatable alloys, in order to benefit from the added effect of Al3Sc-induced hardening, seems the most obvious choice. For instance, the aging temperatures for 2xxx alloys vary between 160 to 190°C, for 6xxx alloys between 160 to 205°C, and for 7xxx alloys between 95 to 180°C. All these temperatures are considerably lower than 350°C, at which the Al3Sc phase in this research is formed. Consequently, adding Sc to non-heat-treatable alloys, such as the 1xxx series (>99% pure Al), the 3xxx series (Al-Mn), and the 5xxx series (Al-Mg), is however promising. These alloys derive their strength from strain hardening and solid solution hardening. Scandium additions to aluminum alloys show promise. Due to the homogeneous distribution of nano-sized Al3Sc precipitates, high strengths can be achieved. The formation of these precipitates increases the hardness by several hundred MPa. Furthermore, these precipitates exert a strong Zener drag on advancing dislocations and grain boundaries, which hinders recrystallization and thereby facilitates the formation of small-grained materials. These alloys differ from other aluminum alloys by their excellent properties at elevated temperatures. The diffusion of Sc in aluminum is low, and consequently, the precipitates coarsen slowly. The strengthening qualities of the Al3Sc phase can be attributed to modulus hardening, coherency hardening, and order

strengthening. Since coherency strengthening may form a major contribution to the hardness of an alloy (Al-Sc alloy), it is important to keep the size of the precipitates below the critical value at which the first misfit dislocation is formed to relieve the misfit strains.

Approximately, this will happen when the number of lattice planes at the grain boundary multiplied by the lattice misfit is equal to one Burgers vector. For the Al-Al3Sc interface, the critical diameter is: dcrit = b/ε = 21.0 nm. However, this critical value will be higher at elevated temperatures due to the larger thermal expansion coefficient of Al and also due to the higher concentration of Sc in solid solution, which will slightly increase the lattice spacing of the matrix. In a deformed microstructure, the precipitation is less homogeneous. Precipitates will then nucleate preferentially on cell walls and individual dislocations. The heterogeneous nucleation effects are more prominent when the aging has been performed at 400°C as compared to aging at lower temperatures. The increased strength is only one of the useful consequences of the formation of the Al3Sc phase. Another aspect is the influence the precipitates have on the recrystallization behavior of the material. It is well-known that randomly distributed precipitates hinder the motion of advancing grain boundaries. This so-called Zener drag can be expressed in the form: pz = k.f/(r), where k is a factor based on the interfacial energy between the dispersoid and the matrix. If, at constant volume fraction, the precipitates coarsen, the Zener drag will decrease rapidly [22].

This drag is such that after the aged microstructure is deformed, the temperature required for recrystallization increases. Clearly, the presence of the precipitates has prevented the recrystallization of the heavily deformed microstructure completely up to temperatures of 550°C. At these temperatures, most of the Sc dissolves in the Al, and the remaining precipitates will coarsen rapidly, minimizing the Zener drag on the boundaries. The Zener drag reaches its maximum for very small precipitates. Even if an annealed microstructure is deformed, after which a recrystallization is attempted, the immediate nucleation of precipitates will prevent this. The deformed microstructure The microstructure of deformed Al specimens consists of screw dislocations arranged in a cell structure. These cells have nearly defect-free interiors and small orientation differences between them. This cell structure is typical for deformed Al specimens and is a result of the high stacking fault energy, which allows screw dislocations to cross-slip easily. At the beginning of the heat treatment, these cells exist, but the precipitates are not yet present. However, the precipitates will nucleate quickly from the solid solution and preserve the cell structure.During precipitation hardening, the interaction between dislocations and obstacles becomes important. The obstacles of primary interest here are precipitates, which include GP zones, metastable second phases, and stable phases. When a dislocation encounters a field of obstacles while moving on a slip plane, it has to choose the path that requires the least energy. It can either move around the particles or through them. In some cases, the dislocation may leave the slip plane in the vicinity of each particle, creating a dislocation ring around each particle through the Orowan mechanism. In either case, the total length of the dislocation line increases, requiring energy input.

The stress required for this process is approximately (Gb)/L, where G is the shear modulus, b is the Burgers vector, and L is the spacing between obstacles.The ageing sequence at temperatures below 190°C typically involves the transformation of α solid solution to GP zones and then to ή and η phases. The ή phase is plate-like, and the η phase is lath or rod-shaped, with both phases considered hexagonal. According to Graf and Schmalzried, GP zones become ordered with Zn and Mg atoms on alternate {100} planes within the zones. The growth kinetics of the two types of particlesdiffer, with particles aged at higher temperatures reaching a metastable equilibrium solute concentration rapidly and undergoing coarsening ($r \propto t1/3$). On the other hand, particles aged at lower temperatures do not reach such a solute concentration and follow a different growth law ($r \propto t1/9$).Stress corrosion cracking (SCC) in Al-Zn-Mg alloys is complex and influenced by numerous parameters. Cracking typically initiates on the surface of a component due to small surface imperfections that generate a fissure, which then propagates through

the component. The process of precipitation hardening directly affects the susceptibility to stress corrosion cracking in high-strength aluminum alloys. These materials are resistant to stress corrosion cracking in the as-quenched state, where grain boundary precipitation is prevented. However, their susceptibility generally increases with increasing precipitation hardening until reaching a maximum before peak strength.

Over-aged heat treatments decrease susceptibility to stress corrosion cracking but also reduce strength. The density of fine precipitates, which contribute to the high strength and stress corrosion cracking resistance of the alloy, is typically controlled by the heat treatment. According to Ward and Lorimer, the Zn content is lower in the precipitate-free zones (PFZ) or remains at the level of the grain interior. A lower Zn content at the grain boundary or in its vicinity during heat treatment reduces the stress corrosion sensitivity of the aluminum alloy. In heat-treatable alloys, precipitation hardening is the dominant mechanism responsible for strength and local strength variations. In friction stir processed materials, all known mechanisms of strengthening of polycrystalline alloys can play a role.

The mechanisms for increasing the critical resolved shear stress (CRSS) of the slip planes are precipitation strengthening, solid solution strengthening, and dislocation strengthening. The response of the polycrystal to stress depends on the CRSS and factors such as local grain size, which can lead to grain boundary strengthening if the grain size is sufficiently small, and crystallographic orientations of grains with respect to each other, namely the crystallographic texture. The chemical composition of the as-cast alloys was determined by ICP-AES and AAS methods and is shown in Table 1. The main constituents of the 7xxx series of Al-Zn-Mg alloys are Zn and Mg. The effect of Zn and Mg on the strength of age-hardened Al-Zn-Mg alloys depends primarily on the Zn + Mg content. The Zn:Mg ratio controls the formation of Zn-bearing constituents. With a ratio greater than 2, MgZn2 (ή) is formed, which contributes to the overall hardening among all phases in the age-hardening process. Impurities such as Fe and Si are mainly responsible for adversely affecting the ageing response and fracture toughness.

The optical micrographs of the studied alloys are shown in Figure 3. Coarsened as-cast grains, dendritic structures, segregation, and eutectic formation on grain boundaries were observed in Alloy-1 and Alloy-2 without Sc addition. However, the minor addition of Sc significantly refined the as-cast grain structure in Alloy-3 and even eliminated the dendritic structure in Alloy-4. The average grain sizes for Alloy-3 and Alloy-4 were measured to be 40.3 μm and 21.7 μm, respectively. In comparison, the as-cast grain sizes for Alloy-1 and Alloy-2 were 50.3 μm and 41.2 μm, respectively. EPMA spot analysis revealed grain boundary segregation of solute atoms in the as-cast Alloy-2 and Alloy-4. Al-Zn-Mg alloys commonly exhibit high volume fractions of alloying elements, resulting in severe dendrite and grain boundary segregation in the grain boundary regions. EPMA analysis showed high solute content in the grain boundary regions of as-cast Alloy-2 and Alloy-4, as confirmed by EDS analysis. The alloys exhibited an equiaxed recrystallized microstructure with homogenized solute concentration and eliminated eutectic phases in the grain boundary regions after solution treatment. The purpose of solution treatment (T4 condition) is to dissolve the coarse equilibrium phases and form a supersaturated solid solution.

This reduces the solute supersaturation of the matrix, decreasing the capabilities of precipitation hardening and lowering strengt of the aluminium alloys [30]. The ageing kinetics has been characterized by Vicker's hardness measurement and activation energy. The activation energies for solute diffusion obtained from the evolution of the Vicker's microhardness. The activation energy (Ea) has been calculated by Arrhenius equation by plotting ln(ΔHV) versus 1/T, the slope of the linear regression fitting indicate activation energy for Alloy-1 and Alloy-4. The values of activation energies of studied alloys has been found out 9.79 kJ/mol (at 10 h ageing time) and 23.73 kJ/mol (at 10 h ageing time), respectively.

The different values of the activation energies indicate that the diffusing species are not same for all alloys [32] . Similarly, the DSC analysis implies precipitation and dissolution of metastable and stable phases in present alloys at heating rate 10°C/min in nitrogen atmosphere. The detailed analysis of DSC data indicates that compositional variations of studied alloying elements have significantly effects the on the formation and dissolution of GP zones, η, ή and T phases [33].

The purpose of solution treatment (i.e., T4 condition) is dissolution of solute elements that will later stage cause of age hardening, spherodization of undissolved constituents and homogenisation of solute concentrations in the materials. Subsequently, quenching is used to retain solute elements in a supersaturated solid solution (SSS) and also create a supersaturated of vacancies that enhance the diffusion and the dispersion of precipitates. Therefore, the size distribution, average size, number density and volume fraction of the Al3Sc particles were determined as a function of the solution treatment temperature and time. Starting from the grain size of the cast aluminium alloys, additions of Sc also increase the resistance to recrystallization during hot working and introduce additional strengthening through the formation of the fine coherent Al3Sc particles from the solid solution. Because the low equilibrium solubility of Sc in the aluminium matrix, these particles precipitates from a supersaturated solid solution during first heat treatment after casting and cannot be dissolved after that, while the strengthening effect depends on their size and number density. Therefore, it is necessary to control precipitation of the Al3Sc particles, in order to achieve the best balance of mechanical properties.

In Figure 5 as solutionizing curve shows Alloy-4 (Sc content 0.83%) best hardness profile throughout the solution heat treatment. Because high Sc content (hypereutectic content, >0.55 Sc, shown in Figure 2) implies greater anti-recrystallization effect and coherent Al3Sc particles main cause of high hardness profile among the present alloys. Similarly, Alloy-1 shows second highest hardness due to higher Zn+Mg contents to effect of solid solution hardening in this heat-treatment phenomenon. The Alloy-2 and Alloy-3 shows moderate hardness profile in this heat treatment phenomena. The artificial ageing has been carried out to all four present alloys to following temperatures at 120°C, 140°C, and 180°C respectively [Figure 6, (a-c)].

During artificial ageing treatment is to make strengthening phases precipitate from the supersaturated solid solution. The precipitation sequence of Al-Zn-Mg alloy is αsss (supersaturated solid solution) →GP zones →metastable ή →stable η. In these three types of precipitates, GP zones and ή metastable phase have strengthening effect on alloy. In the initial stages of ageing treatment, only GP zones and a few ή phases precipitates inside the grains. The strengthening is associated with the shearing GP zones and ή phases by dislocation during deformation. With the longer ageing time, the quantity of GP zones increases, and the strength of alloy increases gradually. In the initial stages of ageing treatment, only GP zones and a few ή phases precipitates inside the grains. The strengthening is associated with the shearing GP zones and ή phases by dislocation during deformation. With the longer ageing time, the quantity of GP zones increases, and the strength of alloy increases gradually.

When the GP zones transform to metastable ή precipitates, the strengthening effect increase with the increase of volume fraction and size. As continuing to extend ageing time, ή phase inside the grains are coarsened gradually, and a part of ή phases transform to η phases. This η phase is incoherent with the matrix and lesser strength to called over-ageing stage. Based on the results and discussion, it can be concluded that strengthening effect of the alloy is associated with the fine strengthening caused by minor additions of Sc, the subgrain strengthening and precipitation strengthening of Al3Sc particles and ή precipitates.

In Figure 6(a) shows Alloy-4 at 120°C ageing phenomena highest hardening effect due to GP zones formation and high density, fine dispersion of Al3Sc precipitates. Similarly, Alloy-1 shows second highest hardening effect due to high solute contests. And Alloy-2, Alloy-3 shows moderate hardening effect at two hours ageing time. In Figure 6 (b) shows Alloy-1 at 140°C ageing phenomena highest hardening effect due to high solute contents to formation of GP -II zones (form above 120°C) and transform to ή phases. Others three alloys in this regime shows lowest ageing response due to transform of η phases, which is noncohe rent with the matrix and resistance effect to dislocation movement is decreased, so strength of alloys decreases. In Figure 6(c) shows Alloy-1 at 180°C ageing phenomena highest hardening effect high solute contents and ή phases transformation. Others three alloys indicate less ageing response in this regime.

This suggests that a phase transformation to η occurs during this period in the overaged stage. The η precipitates are incoherent in the matrix. Hence, the longer interparticle spacing and the coarse size of the η precipitates in the grain result in more reduction in strength. Similarly, FESEM with EDS analysis of as-cast Alloy-2 and Alloy-3 exhibits grain boundary segregation of impurity elements [Figure 7 (a-b)]. In EDS analysis has been shown in both alloys in as-cast conditions grain boundary segregation of solute elements of impurities Fe surplus in Alloy-2 and Sc existence in Alloy-3. In Alloy-2 high Fe content, effects lower strength and ductility in as-cast condition which has been shown in

Table 2. In TEM analysis revealed in as-cast alloys in Figure 8 (a, b), for Alloy-2 dark and white spots indicated GP zones formation and for Alloy-3 precipitates and dislocation interaction observe in present TEM micrograph [33]. In Figure 9 illustrates friction stir processing set-up to cast 7xxx series of aluminium alloys under different heat treatment conditions were subjected to double-passes friction stir processing (FSP). Friction-stir processing has been developed as an effective grain refinement technique based on the principle of friction stir welding.

It is well documented that the intense plastic Deformation and temperature rise during FSP result in the generation of dynamic recrystallization, which produces fine and equiaxed grains in the stirred zone. Essentially, FSP is a local thermo-mechanical metalworking process that changes the local properties without influencing properties in the rest of the structure. During FSP, a specially designed cylindrical tool is inserted into the plate, causing intense plastic deformation through stirring action.

This yields a defect-free, dynamically recrystallized, fine-grained microstructure. Since solid-state friction stir processing does not result in solute loss through evaporation and segregation through solidification, solute elements are homogeneously distributed in the processing zone [34]. Therefore, FSP creates a fine-grained microstructure with dispersively distributed particles and predetermined high-angle grain boundaries. These features are important for enhancing superplastic properties [35].

The tensile specimens for the study were selected from the stir zone according to tensile specifications (gauge length 26 mm, thickness 2.5 mm, width 4 mm, and total length 58 mm). The tensile test results for different heat-treated conditions are tabulated in Table 2. Figure 10(a-d) shows optical micrographs of friction stir processed Alloy-2 from different regions, which identify grain refinement as compared to the unprocessed zones.

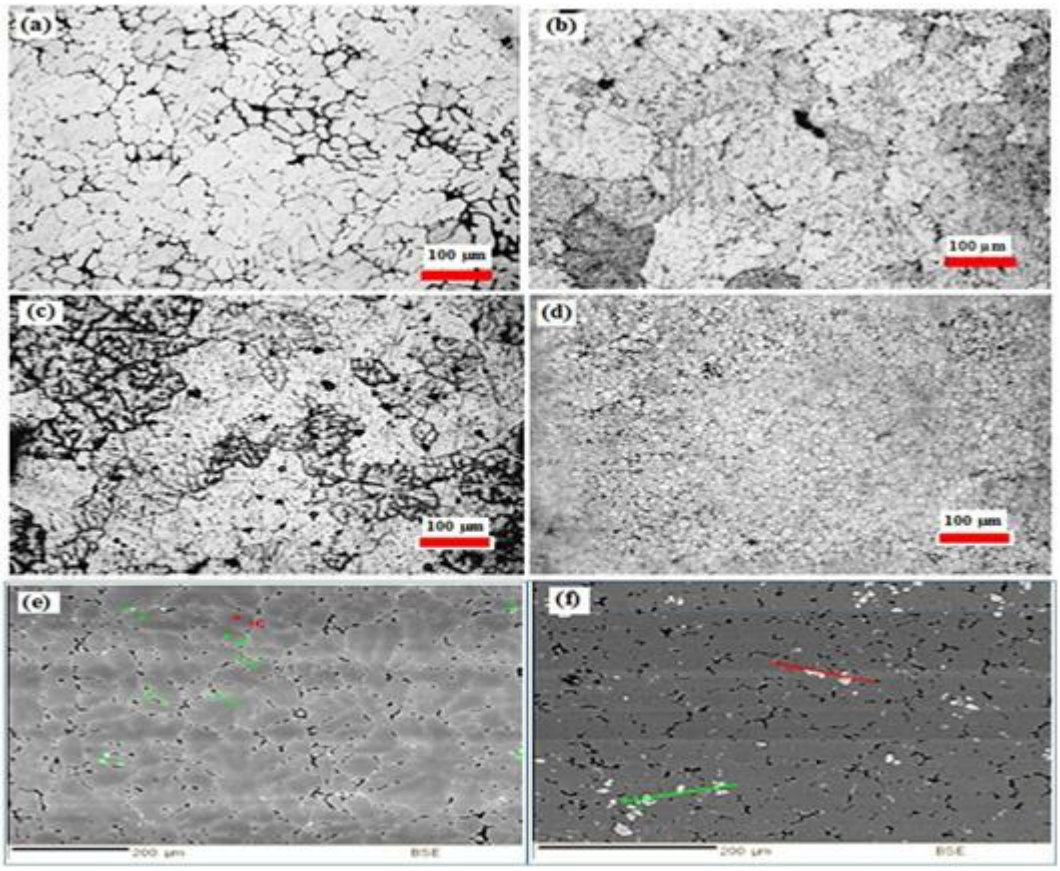

Figure 3. All optical micrographs are as-cast condition : (a) Alloy-1, (b) Alloy-2, (c) Alloy-3, (d) Alloy-4; EPMA micrographs are as-cast condition: (e) Alloy-2, (f) Alloy-4

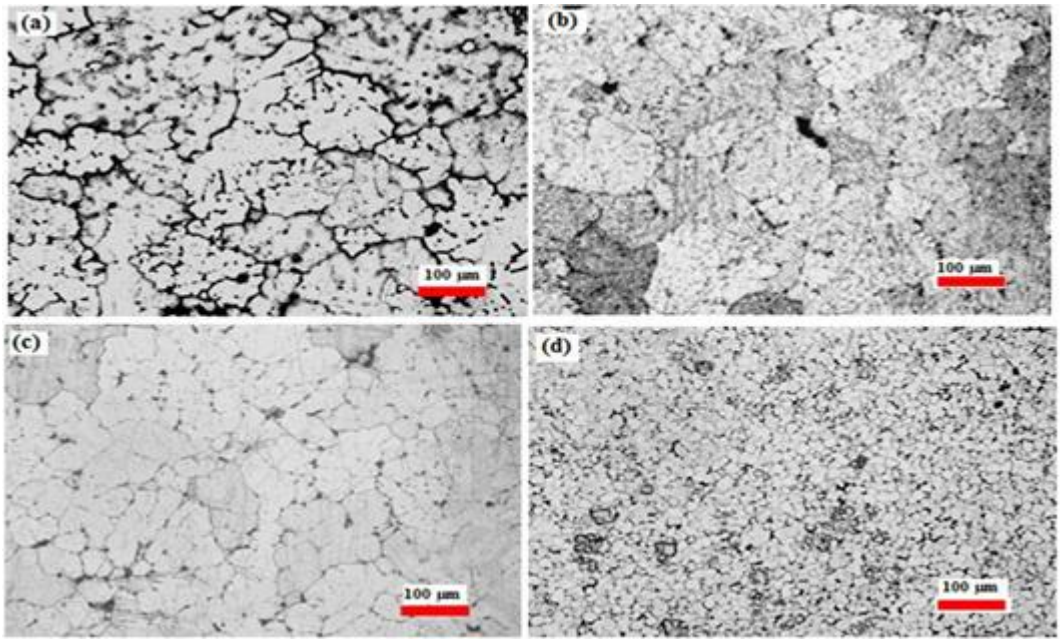

Figure 4. All optical micrographs are T4 condition: (a) Alloy-1, (b) Alloy-2, (c) Alloy-3, (d) Alloy-4

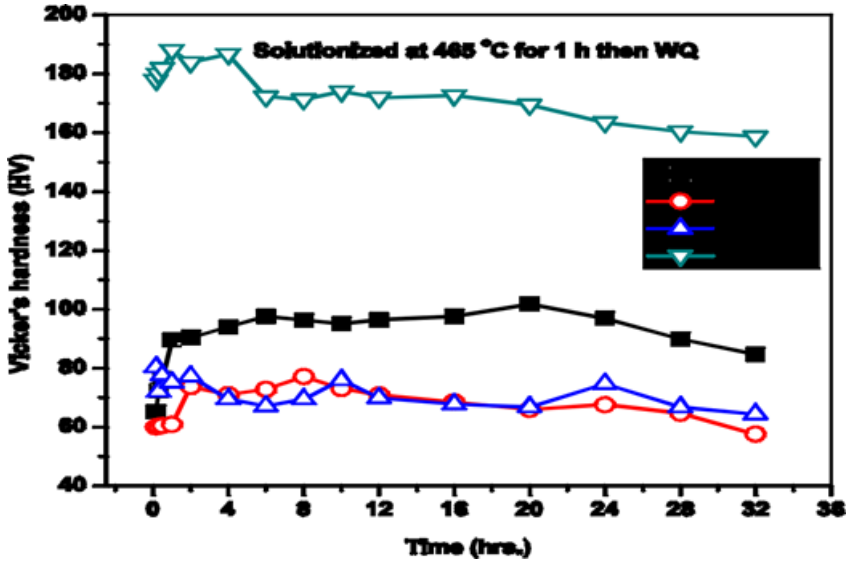

Figure 5. Effect of solutionizing [465°C/1h then immediately water quenched (WQ)] curves on Vicker's hardness of present alloys

Table 1. Chemical composition of prepared aluminium alloys (in wt. %)

Alloy nos.	Chemical composition						Zn+Mg	Zn/Mg ratio
	Zn	Mg	Sc	Si	Fe	Al		
Alloy-1	8.34	3.30	-	0.03	0.04	Balance	11.65	2.52
Alloy-2	6.40	2.50	-	0.05	0.10	Balance	8.90	2.56
Alloy-3	6.70	2.80	0.20	0.023	0.04	Balance	9.50	2.40
Alloy-4	7.10	3.20	0.83	0.01	0.03	Balance	10.30	2.12

Table 2. Results of tensile properties (FSP proceed by double passes and full processed zone)

Alloy no.	As-cast condition			As-cast + FSP			Sol.+FSP			Sol.+FSP+Ageing at 140°C for 2 h		
	$\sigma_{0.2}$ (MPa)	σ_u (MPa)	δ (%)	$\sigma_{0.2}$ (MPa)	σ_u (MPa)	δ (%)	$\sigma_{0.2}$ (MPa)	σ_u (MPa)	δ (%)	$\sigma_{0.2}$ (MPa)	σ_u (MPa)	δ (%)
Alloy-1	35.8	67.5	1.7	72.6	172.9	7.0	133.1	316.8	6.6	113.4	270.0	9.1
Alloy-2	66.3	106.2	2.2	99.2	236.2	6.8	170.5	275.4	9.0	100.6	241.1	5.5
Alloy-3	28.8	49.1	2.0	63.5	141.0	4.7	135.7	251.1	6.0	110.9	264.0	6.9
Alloy-4	89.9	179.8	3.7	115.2	274.3	67.0	165.8	325.3	10.1	168.9	329.0	12.2

*N.B: Solutionized at 465°C/1 h then WQ and yield strength denoted at 0.2% offset from stress-strain curve.

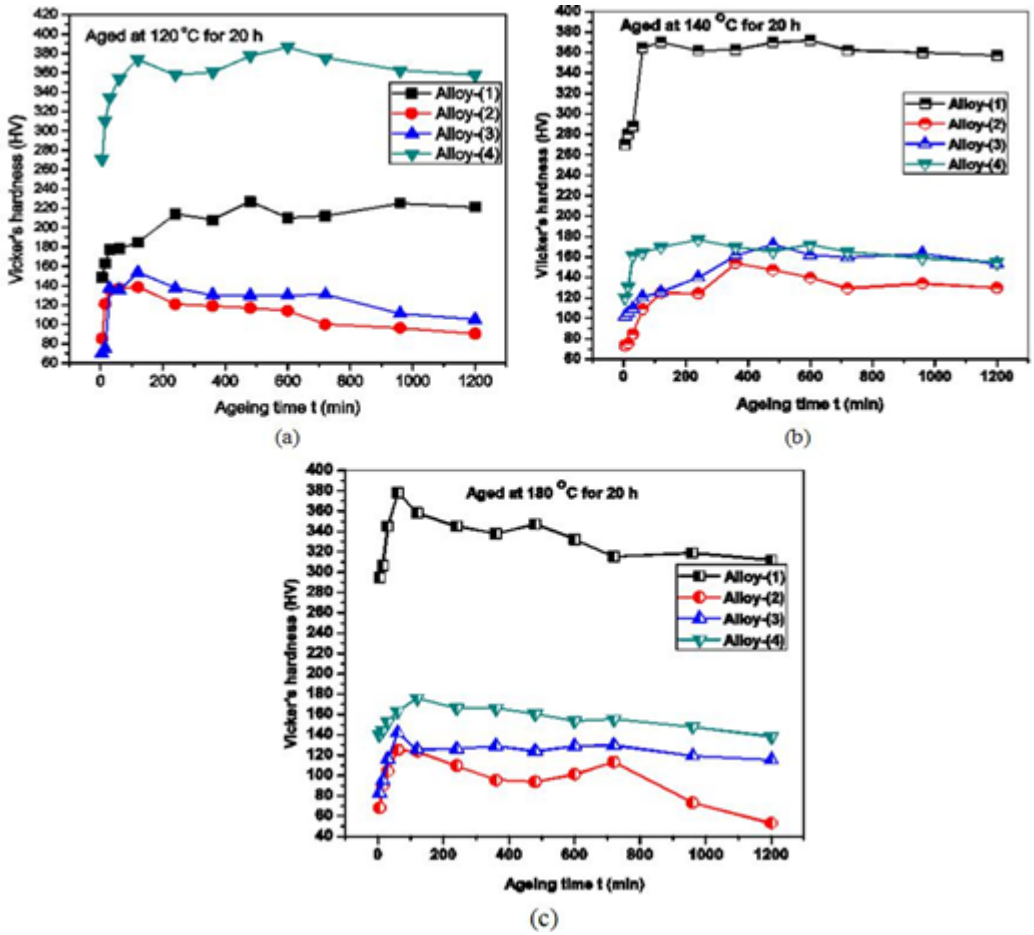

Figure 6. Variation in the Vicker's hardness with ageing time t for the alloys aged at: (a) 120°C, (b) 140°C, and (c) 180°C

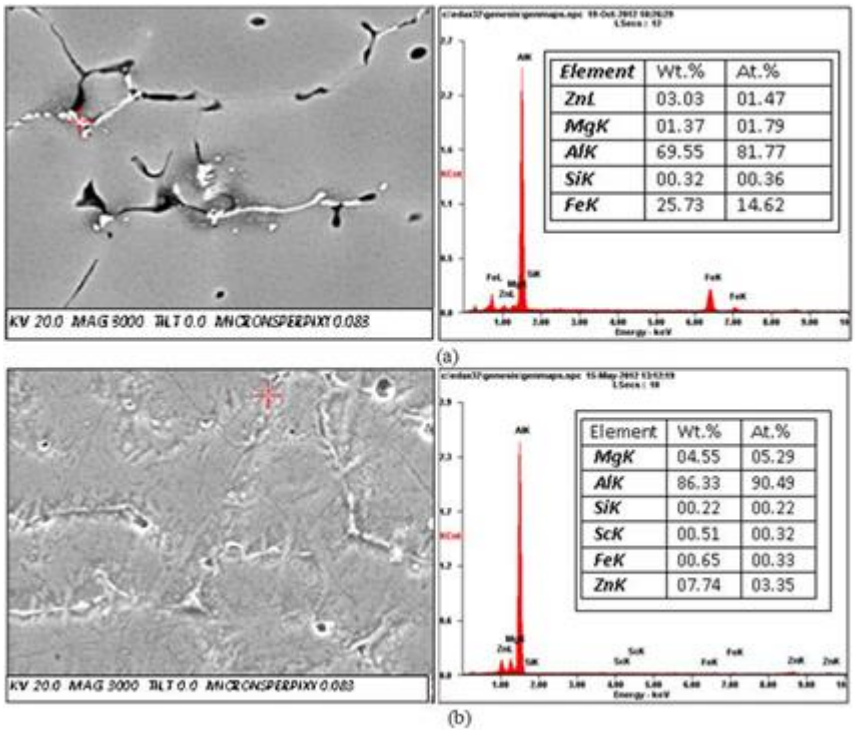

Figure 7. FESEM micrographs and EDS analysis of as-cast condition: (a) Alloy-2; (b) Alloy-3

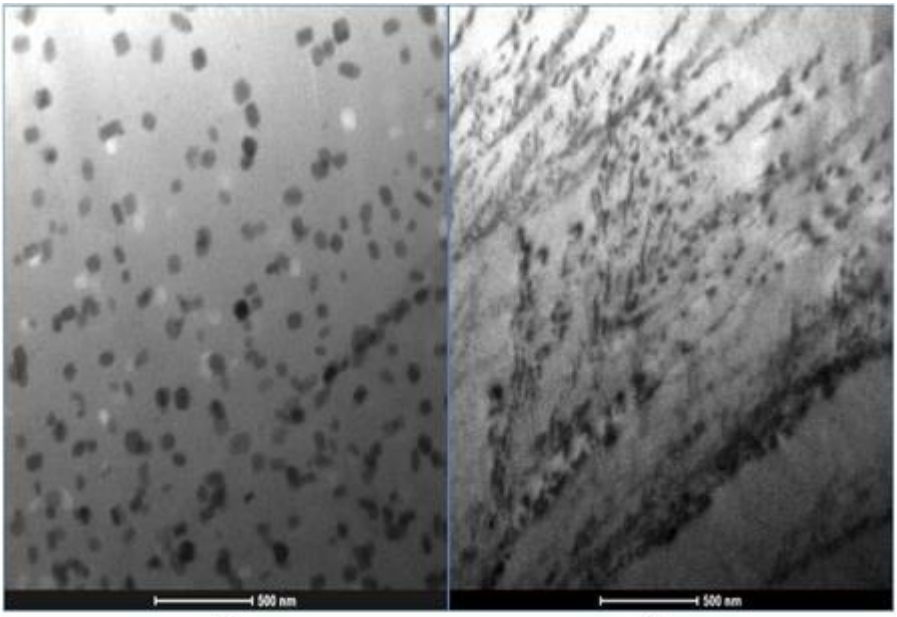

Figure 8. TEM analysis in as-cast condition of: (a) Alloy-2, (b) Alloy-3

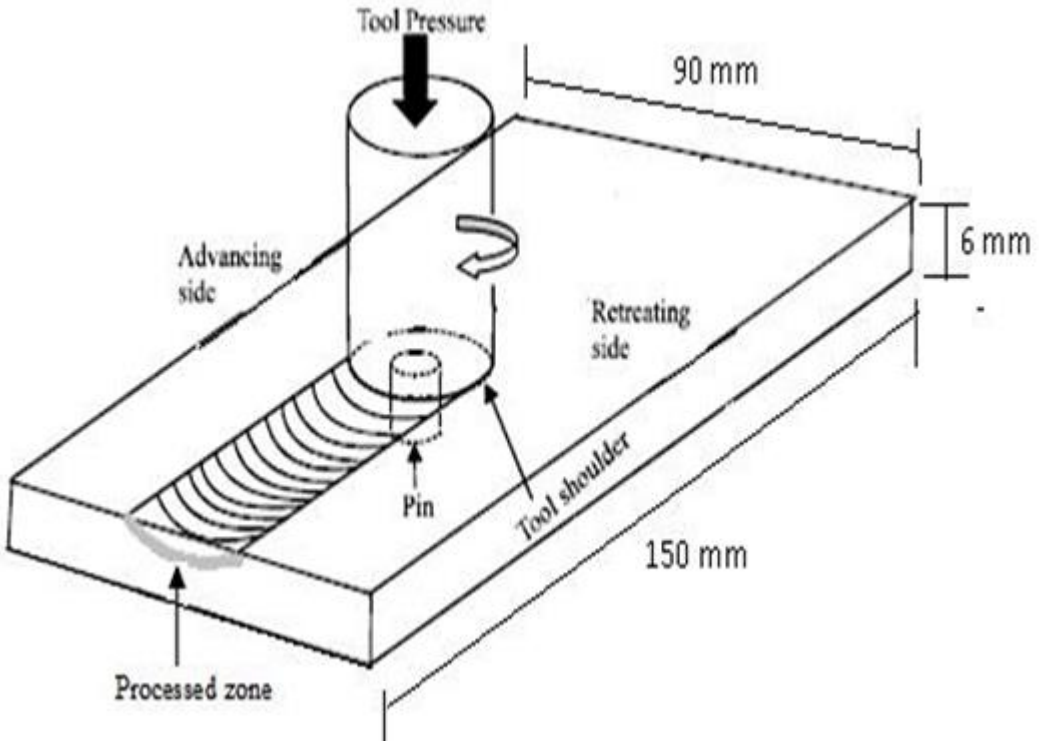

Figure 9. The schematic diagram of friction stir process (FSP) set-up

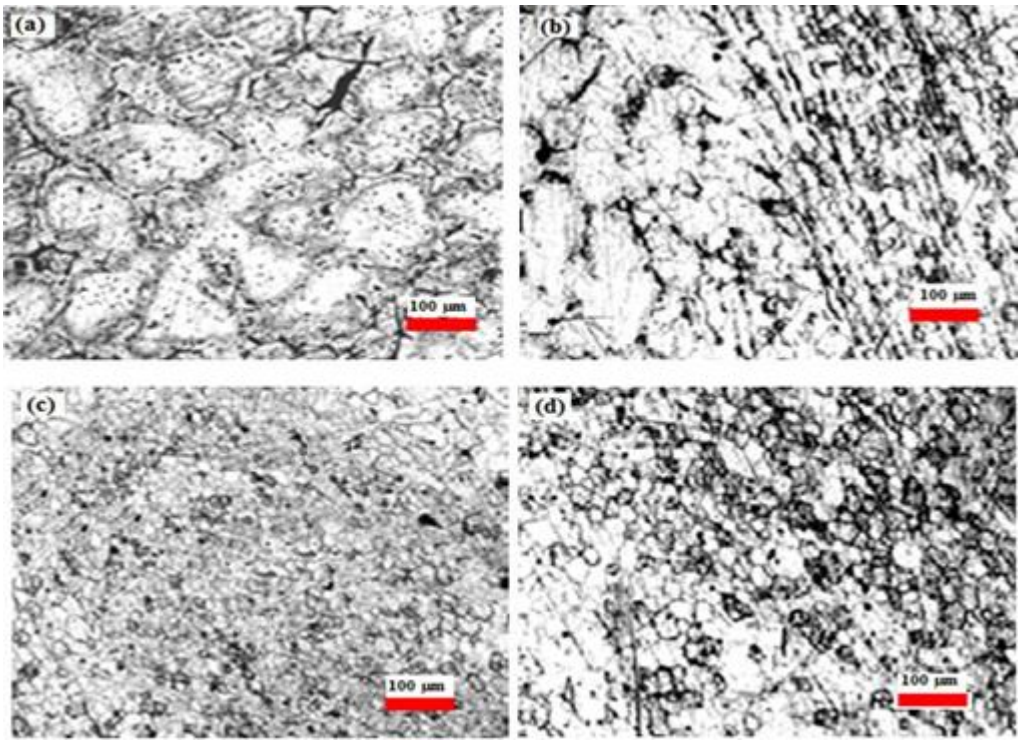

Figure 10. Optical micrographs of Alloy-2 (solutionzed+FSPed): (a) parent metal, (b) process and unprocessed zone (c) nugget zone, (d) recrystallized zone. (1000 rpm and 70 mm/min)

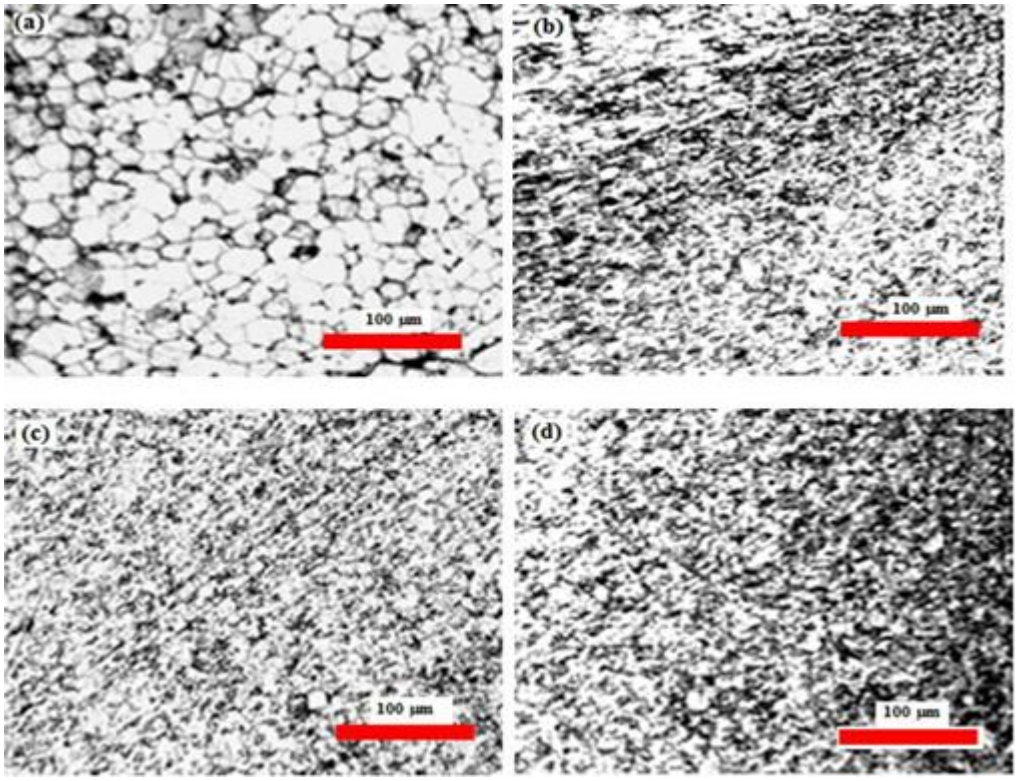

Figure 11. Optical micrographs of Alloy-4 (solutionized+FSPed): (a) parent metal, (b) process and unprocessed zone, (c) nugget zone, (d) recrystallized zone. (1000 rpm and 70 mm/min)

In nugget zone (in Figure 10.(c)) shows very fine grain due to intense plastic deformation and temperature rise during FSP result in the generation of dynamic recrystallization, producing fine and equiaxed grains in the this zone. Similarly, in Figure 11 (a-d) shows friction stir processed Alloy-4 in optical micrographs from different regions identified grain refinement as comparison to unprocessed zones. In nugget zone (in Figure 11(c)) shows fine grain refinement (100-200 nm size) due to frictional heat and dynamic recrystallization and Al3Sc dispersoids balance effects. Since Alloy-4 has very high Sc content (0.84%), so dispersive effect accelerated the increases strength. The tensile test has been performed as different heat treatment conditions as results indicate after FSPed 0.2% proof strength and ultimate tensile strength are increased gradually but specimens with solution heat treated and friction stir processed more enhanced strength and ductility in all four alloys. Due to homogenisation supersaturated solid solution and Al3Sc dispersoid (in cases of Sc added alloys) are more pronounce to fine grain refinement during.

4. CONCLUSIONS:

The 7xxx series of alloys are heat-treatable Al-Zn-Mg alloy. Most ternary alloys are age hard enable. They develop their strength by solution treatment followed by ageing. To addition Sc in Al-Zn-Mg is strong grain-refiner. Eliminated grain boundary segregation, dendritic structure and retarding recrystallization in the as-cast aluminium alloy. In addition Sc to Al-Zn-Mg alloy accelerated ageing kinetics and concentrated GP zones formation. The addition of Sc improves the mechanical properties of the alloys. The reason is the precipitation of secondary Al3Sc particles and the remarkable refinement of the grains, namely, precipitation strengthening and fine-grain strengthening. The higher ductility is due to the elimination of porosity and the breakup of coarse second phase particles. The tensile strength after FSP has been improved due to grain refinement and homogenization of precipitates particles of present aluminium alloys. However, the frictional heat and severe plastic deformation and the residual stresses are prime mechanisms to enhanced strength of present aluminium alloys In the as-cast state the strength of the supersaturated solid solution increases with increasing Zn and Mg content due to solid solution hardening. However, after FSP the work hardening and Hall-Patch hardening due to the decreasing grain size competes with softening due to the decomposition of a supersaturated solid solution. In the net effect, theFSP results in a softening of aluminium alloys. Dispersoids like Al3Sc are effective means of inhibiting the grain growth during FSP.

REFERENCE:

[1] W. Jurczak, “The effect of heat treatment on the structure and corrosion resistance of Al-Zn-Mg alloys”, POLISH MARITIME RESEARCH, 4(58) 2008 Vol. 15, pp. 66-71.
[2] F. Xi-gang, J. Da-ming, M. Qing-chang, Z. Bao-you, W. Tao, “Evolution of eutectic structures in Al-Zn-Mg-Cu alloys during heat treatment”, Transactions of Nonferrous Metals Society of China, 16 (2006), pp. 577-581.
[3] W.J. Poole, J.A. Saeter, S. Skjervold, G. Waterloo, “A Model for Predicting the Effect of Deformation after SolutionTreatment on the Subsequent Artificial Aging Behavior of AA7030 and AA7108 Alloys”, Metallurgical and Materials Transactions A, Vol. 31A, September 2000, pp. 2327-2338.
[4] L. Wen-bin, P. Qing-lin, X. Yan-ping, H. Yun-bin, L. Xiao-yan, “Microstructural evolution of ultra-high strength Al-Zn-Cu-Mg-Zr alloy containing Sc during homogenization”, Transactions of Nonferrous Metals Society of China, 21 (2011), pp. 2127-2133.
[5] A. Dupasquier, R. Ferragut, M.M. Iglesias, C. E. Macchi, “Early solute clustering in an AlZnMg alloy”, Materials Science Forum, Vols. 445-446 (2004), pp. 16-20.

[6] W. Feng, X. Baiqing, Z. Yongan, Z. Baohong, "Age-hardening characteristic of an Al-Zn-Mg-Cu alloy produced by spray deposition", RARE METALS, Vol. 26, No. 2, April 2007, pp. 163-168.
[7] R. Ferragut, A.Somoza, A. Dupasquier, "Positron lifetime spectroscopy and decomposition processes in commercial Al-Zn- Mg-based alloys", J. Phys.: Condens. Matter 10 (1998), pp. 3903-3918.
[8] G. Sha, A. Cerezo, "Early-stage precipitation in Al-Zn-Mg-Cu alloy (7050)", Acta Materialia, 52 (2004), pp. 4503-4516.
[9] H. Inoue, T. Sato, Y. Kojima, T. Takahashi, "The Temperature Limit for GP Zone Formation in an Al-Zn-Mg alloy", Metallurgical Transaction A, Vol. 12A, August 1981, pp. 1429-1434.
[10] C. E. Lyman, J. B. Vander Sande, "A Transmission Electron Microscopy Investigation of the Early Stages of Precipitation in an Al-Zn-Mg Alloy", Metallurgical Transaction A, Vol. 7A, August 1976, pp. 1211-1216.
[11] H. Loffler, I. Kovacs, J. Lendvai, "Review Decomposition processes in Al-Zn-Mg alloys", Journal of Materials Science 18 (1983), pp. 2215-2240.
[12] B.A. Parker, Z.F. Zhou, P. Nolle, "The effect of small additions of scandium on the properties of aluminium alloys", Journal of Materials Science, 30 (1995), pp. 452-458.
[13] H. Yong-dong, Z. Xin-ming, Y. Jiang-hai, "Effect of minor Sc and Zr on microstructure and mechanical properties of Al- Zn-Mg-Cu alloy", Transactions of Nonferrous Metals Society of China, 16 (2006), pp. 1228-1235.
[14] X. Dai, C. Xia, A. Wu, X. Peng, "Influence of Scandium on Microstructures and Mechanical Properties of Al-Zn-Mg-Cu-Zr Alloys", Materials Science Forum, Vols. 546-549, (2007), pp. 961-964.
[15] V.G. Davydov, T.D. Rostova, V.V. Zakharov, Y.A. Filatov, V.I. Yelagin, "Scientific principles of making an alloying addition of scandium to aluminium alloys", Materials Science and Engineering A280 (2000), pp. 30-36.
[16] Y.W.Riddle, T.H. Sanders, Jr., "A Study of Coarsening, Recrystallization, and Morphology of Microstructure in Al-Sc- (Zr)-(Mg) Alloys", Metallurgical and Materials Transactions A, Vol. 35A, January 2004, pp. 341-350.
[17] V. V. Zakharov, "EFFECT OF SCANDIUM ON THE STRUCTURE AND PROPERTIES OF ALUMINUM ALLOYS", Metal Science and Heat Treatment, Vol. 45, Nos. 7-8, 2003, pp. 246-253.
[18] T.R Ramachandran, P.K.Sharma, K. Balasubramanian, "Grain Refinement of Light Alloys", 68th WFC- World Foundry Congress, 7th-8th February, 2008, pp. 189-193.
[19] M. Enescu, I. Popescu, R. Zamfir, A. Molagic, V. Bratu, "Experimental researches on the corrosion behaviour and microstructural aspects of heat treated Al-Zn-Mg-Cu alloys", INTERNATIONAL JOURNAL of ENERGY and ENVIRONMENT, Issue 4, Vol. 4, 2010, pp. 122-130.
[20] F. Nascimento, T. Santos, P. Vilaca, R.M. Miranda, L. Quintino, "Microstructural modification and ductility enhancement of surfaces modified by FSP in aluminium alloys", Materials Science and Engineering A 506 (2009), pp. 16-22.
[21] Y.J. Kwon, N. Saito, I. Shigematsu, "Friction stir process as a new manufacturing technique of ultrafine grained aluminium alloy", Journal of Materials Science Letters 21, 2002, pp.1473-1476.
[22] J.Royset, N. Ryum, "Scandium in aluminium alloys", International Materials Reviews, Vol.50, No.1, pp. 19-44.
[23] C.E. Lyman, J.B. Vander Sande, "A transition electron microscopy investigation of the early stages of precipitation in an Al-Zn-Mg alloy", Metallurgical Transaction A, Vol.7A, Aug 1976, pp. 1211-1216.
[24] L. Wu, W. Wang, Y. Hsu, S. Trong, Effects of Microstructure on the Mechanical Properties and Stress Corrosion Cracking of an AlZn-Mg-Sc-Zr Alloy by Various Temper Treatments, Materials Transactions, Vol. 48, No. 3 (2007), pp. 600- 609.

[25] A. Csanandy, D. Marton, Stress corrosion behaviour of Al-Zn-Mg alloys based upon microchemical surface reactions,Journal of Materials Science 14 (1979), pp. 2289-2295.
[26] A. V. Sameljuk, O. D. Neikov, A.V. Krajnikov, Y. V. Milman, G. E. Thompson, Corrosion behaviour of powder and cast Al-Zn-Mg base alloys, Corrosion Science 46 (2004), pp. 147-158.
[27] M J Starink, A Deschamps, S C Wang, "THE HIGH STRENGTH OF FRICTION STIR WELDED AND FRICTION STIR PROCESSED ALUMINIUM ALLOYS", Scripta Materialia 58 (2008), pp. 377-382.
[28] L.F. Mondolfo, "Aluminium alloys: structure and properties", Butterworth, London, 1976.
[29] B.B. Gupta, A.K. Mallik, "Comparative Aging Behavior of Commercial and High Purity Al-Zn-Mg Alloy", Trans. JIM, Vol.5, 1975, pp. 779-786.
[30] L. Wu, W. Wang, Y. Hsu, S. Trong, "Effects of homogenization treatment on recrystallisation behaviour and dispersoid distribution in an Al-Zn-Mg-Sc-Zr alloy", Journal of Alloys and Compounds 456 (2008), pp. 163-169.
[31] W.Sha, "Activation energy for precipitation hardening and softening in aluminium alloys calculated using hardness and resistivity data,
[32] K.S. Ghosh, N. Gao, "Determination of kinetics parameters from calorimetric study of solid state reactions in 7150 Al-Zn- Mg alloy", Transactions of Nonferrous Metals Society of China, 21 (2011), pp. 1199-1209.
[33] F.C. Liu, Z.Y. Ma, "Achieving high strain rate superplasticity in cast 7075Al alloy via friction stir processing," Journal of Materials Science, (2009) 44, pp. 2647-2655.
[34] C.M Hu, C.M. Lai, P.W. Kao, N.J. Ho, J.C. Huang, "Quantitative measurements of small scaled grain sliding in ultra-fine grained Al-Zn alloys produced by friction stir processing", Materials Characterisation 61 (2010), pp. 1043-1053.
[35] G.R. Cui, Z.Y. Ma, S.X. Li, "The origin of non-uniform microstructure and its effects on the mechanical properties of a friction stir processed Al-Mg alloy", Acta Materialia57 (2009), pp. 5718-5729